DOI:
10.1016/j.jacc.2016.10.058

Document Version
Peer reviewed version

Diabetes Mellitus-induced Microvascular Destabilization in the Myocardium

Rabea Hinkel, DVM,[a,b,c] Andrea Hoewe, DVM,[a] Simone Renner, DVM,[d,e] Judy Ng, PHD,[a] Seungmin Lee, PHD,[a] Katharina Klett, DVM,[a,c] Veronika Kaczmarek, MD,[a,c] Alessandra Moretti, PHD,[a,b] Karl-Ludwig Laugwitz, MD, [a,b] Philipp Skroblin, PHD,[f] Manuel Mayr, MD,[f] Hendrik Milting, MD,[g] Andreas Dendorfer, MD,[h] Bruno Reichart, MD,[h] Eckhard Wolf, DVM,[d,e] Christian Kupatt, MD[a,b,h]

[a]I. Medizinische Klinik und Poliklinik, University Clinic Rechts der Isar, TUM and
[b]DZHK (German Center for Cardiovascular Research), partner site Munich Heart Alliance, Munich, Germany
[c]Institute for Cardiovascular Prevention, KUM Munich, Germany
[d]Chair for Molecular Animal Breeding and Biotechnology, Gene Center and Department of Veterinary Sciences, LMU Munich, Germany
[e]German Center for Diabetes Research (DZD), Neuherberg, Germany
[f]Kings College London BHF Centre, United Kingdom
[g]Erich & Hanna Klessmann Institute, Heart and Diabetes Center Northrhine Westphalia, Bad Oeynhausen, Germany
[h]Walter-Brendel-Centre for Experimental Medicine, LMU Munich, Germany

Acknowledgements: This work was funded by the German Research Foundation (DFG, TRR 127 to RH, CK, BR and EW), the German Center for Cardiovascular Research (DZHK), the German Center for Diabetes Research (DZD), and the German Ministry for Education and Research (BMBF 01GU1105 to CK). We wish to thank Anja Wolf for expert technical assistance.
Disclosures: None of the authors has a conflict of interest to declare

[*]**Corresponding Address:**
Christian Kupatt, MD
1. Med. Klinik, University Clinic Rechts der Isar
Technical University Munich
Ismaninger Str. 22
81675 Munich, Germany
Telephone: +49-89-4140-9086
Fax: 0049-89-4140-4901
E-mail: Christian.kupatt@tum.de

ABSTRACT

BACKGROUND Diabetes mellitus causes microcirculatory rarefaction and may impair the responsiveness of ischemic myocardium to proangiogenic factors.

OBJECTIVES We sought to determine whether microvascular destabilization affects organ function and therapeutic neovascularization in diabetes mellitus.

METHODS We obtained myocardial samples from patients with end-stage heart failure at time of transplant, with or without diabetes mellitus. Diabetic (db) and wild-type (wt) pigs were used to analyze myocardial vascularization and function. Chronic ischemia was induced percutaneously (day 0) in the circumflex artery. At day 28, recombinant adeno-associated virus (rAAV, 5 x 10^{12} viral particles encoding vascular endothelial growth factor-A [VEGF-A] or Thymosin β4 [Tβ4]) was applied regionally. $CD31^{+}$ capillaries per high power field (c/hpf) and $NG2^{+}$ pericyte coverage (p/hpf) were analyzed. Global myocardial function (ejection fraction [EF] and left ventricular end-diastolic pressure) was assessed at days 28 and 56.

RESULTS Diabetic human myocardial explants revealed capillary rarefaction and pericyte loss compared to nondiabetic explants. Hyperglycemia in db pigs, even without ischemia, induced capillary rarefaction in the myocardium (163 ± 14 c/hpf in db vs. 234 ± 8 c/hpf in wt hearts; $p < 0.005$), concomitant with a distinct loss of EF (44.9% vs. 53.4% in nondiabetic controls; $p < 0.05$). Capillary density further decreased in chronic ischemic hearts as did EF (both $p < 0.05$). Treatment with rAAV.Tβ4 enhanced capillary density and maturation in db hearts less efficiently than in wt hearts, similar to collateral growth. rAAV.VEGF-A, though stimulating angiogenesis, did not induce pericyte recruitment nor collateral growth. As a result, rAAV.Tβ4 but not rAAV.VEGF-A improved EF in db hearts (34.5 ± 1.4%), but less so than in wt hearts (44.8 ± 1.5%).

CONCLUSIONS Diabetes mellitus destabilized microvascular vessels of the heart, affecting the amplitude of therapeutic neovascularization via rAAV.Tβ4 in a translational large animal model of hibernating myocardium.

KEY WORDS angiogenesis, chronic myocardial ischemia, gene therapy, Thymosin ß4

ABBREVIATIONS AND ACRONYMS

Ang = angiopoietin
db = diabetic
hpf = high power field
LVEDP = left ventricular end-diastolic pressure
miR = micro ribonucleic acid
rAAV = recombinant adeno-associated virus
RCx = ramus circumflexus
Tβ4 = thymosin beta 4
VEGF-A = vascular endothelial growth factor A
wt = wild type

Diabetes mellitus (DM) is one of the most important risk factors for developing cardiovascular disease (1,2). Moreover, DM induces additional major adverse coronary events after percutaneous coronary interventions (3-6) and bypass grafting, particularly if poorly controlled (7). This comparative disadvantage is also evident when interventions are performed for acute coronary syndromes (8) and for chronic coronary lesions, aimed at resolving contractile dysfunction in viable myocardium (i.e., hibernating myocardium) (9,10).

Apparently, macrovascular treatment options for coronary obstructions are antagonized by additional factors beyond the reach of conventional recanalization strategies (11). A continuous inflammatory disposition of microvessels has been attributed to vessel regression in most organs (12), except for reactive inflammatory vessel growth in the eye (13). Both rarefaction and capillary sprouting imply vessel destabilization as a common denominator. In this concept, pericyte detachment is caused by inflammatory endothelial activation (13). The diabetic inflammatory process might be aggravated by exogenous vessel-destabilizing factors such as vascular endothelial growth factor (VEGF)-A (14), potentially blunting its efficacy in therapeutic neovascularization. Enhancing microvascular stability (e.g., by providing platelet-derived growth factor B for pericyte attraction), has been demonstrated to increase blood flow into ischemic myocardium, when added to VEGF-A (15). One vascular growth factor, which provides both capillary sprouting and pericyte investment, is Thymosin β4 (Tβ4) (16), which induces lasting and functional microvascular networks in wild-type (wt) animals, and stabilizes microvessels in the instance of inflammation (17).

To determine whether microvascular destabilization affects organ function and therapeutic neovascularization in a clinically relevant large animal model, we studied ischemic cardiomyopathy in *INS*^{C94Y} transgenic pigs, a model of permanent neonatal DM (18). In this

model, fasting glucose levels increased to 300 to 400 mg/dl after birth. We analyzed hearts of 5-month-old diabetic (db) and wt pig hearts with or without hibernating myocardium, and applied regional adeno-associated virus (AAV)-based vascular gene therapy in the latter. Our results indicated that molecular treatment aiming at balanced vascular growth and maturation can improve hibernating myocardium in individuals with DM, although to a lesser extent than in age-matched non-DM controls.

METHODS

Tissue samples of the nonischemic and ischemic animals (ramus circumflex [RCx] perfused area, wt and db) and patient samples (5 in the non-DM and 4 in the DM group, left ventricle [LV], ischemic area) were analyzed for capillary density (platelet endothelial cell adhesion molecule [PECAM]-1 positive cells) and pericyte investment (NG2 positive cells). More information about tissue staining is in the **Online Appendix**.

Myocardial tissue specimens were procured from patients undergoing heart transplantation (**Online Table 1**). Patients provided informed consent for the scientific use of the explanted tissue. The study was approved by the institutional ethics boards of the clinical and experimental study contributors (H.M., A.D.). Specimens of LV myocardium (4 in the non-DM and 5 in the DM group) were obtained as 2 x 2 cm^2 transmural biopsies from explanted failing hearts at the Heart and Diabetes Center of Northrhine Westphalia, and were prepared as described in the **Online Appendix**.

Isometric contraction force was measured at a preload of 1 mN under continuous field stimulation (rate 0.5 Hz, pulse duration 3 ms) at 1.5-fold excitation threshold. Strain- and rate-related alterations of contractility were determined in the presence of 1 μM isoprenaline.

Maximum twitch force was assessed at optimum preload. Tissue elastance was calculated from the increase in diastolic tension provoked by a 1 mm extension beyond relaxed length.

The preparation of cells for direct matrigel assays, pericyte coculture experiments, and shear stress experiments is described in the **Online Appendix**.

Recombinant AAV (rAAV)2.9 vectors encoding ß-galactosidase lacZ, Tβ4, or VEGF-A were produced using the triple transfection method as described earlier (19) and in the **Online Appendix**.

Transgenic pigs presenting with permanent neonatal DM were generated as described previously (18). The *INS*^{C94Y} mutation disrupts 1 of the 2 disulfide bonds between the A and B chains of the insulin molecule, resulting in misfolded insulin, impaired insulin secretion, endoplasmic reticulum stress, and apoptosis of the pancreatic beta cells. Consequently, these transgenic pigs present with permanent neonatal DM, which was treated with insulin until 7 days before experiment onset. Healthy nontransgenic littermates served as controls (**Online Figure 1A**).

German landrace pigs were anesthetized and instrumented as previously described (20) and in the **Online Appendix**. Of 37 animals initiated by stent placement, 5 (3 wt and 2 db) were lost due to sudden cardiac death during the first 28 days, whereas no animal was lost between days 28 and 56. The remaining 32 animals (14 wt, 18 db) were treated by mock transduction (5 x 10^{12} rAAV containing no transgene; n = 7 wt, n = 6 db), rAAV.VEGF-A transduction (5 x 10^{12} particles; n = 5 db), or rAAV.Tβ4 tranduction (5 x 10^{12} particles; n = 7 wt and db) via continuous pressure-regulated retroinfusion into the lateral vein (21).

Twenty-eight days after implantation of a reduction stent, the myocardium was transduced with Tβ4 or VEGF-A by selective pressure regulated retroinfusion of 5 x 10^{12}

rAAV.Tβ4 or $1x10^{13}$ rAAV.VEGF-A particles into the lateral vein, which anatomically drains the RCx-perfused myocardium (15) (**Online Figure 1B).** Four weeks later (day 56), we assessed collateral morphology and myocardial function as well as performed tissue harvesting for histochemical analysis.

Global myocardial function was assessed at days 28 and 56 by means of a pressure-tip catheter placed in the left ventricle (for LV end-diastolic and systolic pressures, dP/dt_{max}, and dP/dt_{min}), whereas LV angiography was performed in anterior-posterior position for the analysis of ejection fraction (EF), yielding slightly smaller control values than a right anterior oblique view. At day 56, subendocardial segment shortening (SES) was performed after placing sonomicrometry crystal pairs into the ischemic (Cx-perfused) region and normalized to measurements in the control region (left anterior descending artery perfused area). Though 1 animal of the treatment group died during SES assessment, it provided all other data.

Post-mortem angiograms were taken for visualization of collateral formation and Rentrop score analysis: 0 = no filling; 1= side branch filling; 2 = partial main vessel filling; and 3 = complete main vessel filling. Tissue from nonischemic and ischemic LV myocardium was utilized for determining capillary density.

STATISTICAL METHODS. The results are given as mean ± SE of the mean (SEM). Statistical analysis of results between more than 2 experimental groups was performed with 1-way analysis of variance (ANOVA) in **Figures 1B, 2B, 2C, 4B, and 4C**; 2-way ANOVA was applied in all other figures that compared more than 2 groups and more than 1 condition. Whenever a significant effect was obtained with ANOVA, we performed multiple comparison tests between the groups using the Student Newman-Keule procedure. Two experimental groups were compared by Student *t* test. All procedures were performed with an SPSS Version 19.0.2

(IBM Corporation, Armonk, New York). Differences between groups were considered significant at $p < 0.05$.

RESULTS

Although diabetic microvascular alterations are well-known in peripheral or retinal tissue of patients, data are scarce that describe a structure-function correlation in diabetic hearts. Therefore, we first compared myocardium of end-stage hearts from patients with and without DM undergoing heart transplantation, utilizing specimens of freshly explanted hearts for histological and functional analyses. We found a distinct capillary rarefaction and pericyte loss in hearts derived from patients with DM (**Figures 1A through 1C**), accompanied by a lowered angiopoietin (Ang)1/Ang2 ratio in the DM group (**Figure 1D**). This microvascular alteration coincided with a loss of contractility in the papillary muscle ex vivo (**Figure 1E**). Moreover, wall stiffness, a parameter for impaired ventricular filling indicating diastolic heart failure, was found increased in the same hearts (**Figure 1F**), all confirming a correlation between microvascular disturbance and dysfunction in hearts from DM patients.

Next, we investigated the impact of increased glucose levels on sprouting and maturation of endothelial cells in vitro. We used 2 well-known pro-angiogenic stimuli, VEGF-A and Tβ4 (16), to induce tube formation of microvascular endothelial cells (bEnd3 and human umbilical venous endothelial cells). Under normal glucose conditions, cells displayed a high spontaneous tube formation rate, which was almost 2-fold increased upon Tβ4 stimulation (**Figure 2A**). Tube formation was reduced at high glucose concentration (61% of cells at normal glucose), but increased to 174% upon Tβ4 and 162% upon VEGF-A stimulation (**Figure 2A**). Consistently, Tβ4 enhanced the migratory capacity of endothelial cells in vitro in both normo- and high-glucose conditions, although to a lesser extent in the high-glucose culture condition (**Figure 2B**).

Of note, while Tβ4 increased pericyte recruitment to the newly formed capillary rings at normal and high-glucose conditions, adding VEGF-A did not alter pericyte recruitment and high-glucose conditions impaired the capability of endothelial cells to attract pericytic cells to newly formed capillary rings (**Figures 2C and 2D**).

The proangiogenic endothelial activation of Tβ4 under normal and high-glucose conditions did not induce pro-inflammatory events, since adhesion of monocytic THP-1 cells to endothelial cells decreased in both conditions upon Tβ4 treatment (**Figure 2E**). Nevertheless, adhesion of THP-1 cells on endothelial cells was found increased at high compared to normal glucose levels, pointing to a chronic inflammatory state of diabetic endothelium (**Figure 2E**).

Next, we investigated the impact of high glucose levels on the microcirculatory status and myocardial function in otherwise unchallenged hearts in vivo. Noteworthy, at 5 months of age with blood glucose levels >300mg/dl (**Figure 3A**), a distinct capillary rarefaction was detectable in normoxic db pig hearts (163 ± 14 vs. 234 ± 8 capillaries/high power field [c/hpf] in wt) (**Figures 3B and 3C**). Moreover, pericyte investment of the remaining capillaries was decreased, rendering the microcirculatory networks in nonischemic hearts impaired (144 ± 6 vs. 219 ± 4 pericytes [p]/hpf) (**Figures 3B and 3D**). Coincidentally, an increase in interstitial fibrosis was noted in db hearts (15.6 ± 0.6% vs.2.1 ± 0.5%) (**Figures 3E and 3F**). This structural alteration was associated with an impairment of systolic parameters such as EF (44.9 ± 1.9 % in db vs. 53.4 ± 1.2 in wt hearts) (**Figure 3G**). Consistently, db hearts demonstrated a decrease in functional reserve (6.6 ± 1.3% vs. 15.4 ± 2.3% at 150 beats/min) (**Figure 3H**) as well as an increase of LV end-diastolic pressure (12.7 ± 1.0 mm Hg vs. 8.2 ± 0.7 mm Hg) (**Figure 3I**).

In a second set of experiments, we analyzed the response of diabetic porcine hearts (blood glucose >300 mg/dl) (**Figure 4A**) and age-matched control hearts subjected to regional

chronic ischemia inflicted by gradual occlusion of the circumflex artery. We found a higher degree of microcirculatory rarefaction in diabetic than in normoglycemic hibernating myocardium (129 ± 7 vs. 150 ± 4 c/hpf) (**Figures 4B and 4C**). Pericyte investment of capillaries was also decreased in diabetic hearts (106 ± 4 p/hpf vs. 136 ± 5 p/hpf) (**Figures 4B through 4D**). Of note, rAAV.Tβ4 transduction significantly induced capillary growth and maturation in diabetic pigs (183 ± 9 c/hpf, 163 ± 14 p/hpf), although less pronounced than in wt hearts (294 ± 6 capillaries/hpf, 286 ± 7 p/hpf; **Figures 4B through D**). Treatment of diabetic hearts with rAAV.VEGF-A treatment yielded an increase in capillaries (192 ± 4 c/hpf) **Figures 4B and 4C**). However, the pericyte investment did not concomitantly increase (87 ± 4 p/hpf) (**Figures 4B and 4D**).

The number of collaterals, which may be formed to compensate for chronic total RCx occlusion, was low in both db and wt groups (2.1 ± 0.5 vs. 1.9 ± 0.2 visible collaterals per heart) (**Figures 4E and 4F**). Upon rAAV.Tβ4 transduction, however, collateral formation increased to a larger extent in wt hearts (6.7 ± 0.5 collaterals/heart) than in diabetic hearts (4.7 ± 0.3 collaterals/heart) (**Figures 4E and 4F).** Consistently, Rentrop score indicating distal filling of the occluded vessel reached a higher level wt hearts than in db hearts (2.6 ± 0.2 vs. 2.1 ± 0.1) (**Figures 4E and 4G**). Notably, rAAV.VEGF-A treatment did not increase arteriogenesis in the ischemic region of diabetic hearts (2.2 collaterals/heart,), with a Rentrop score at control level (rAAV.VEGF-A 1.2 ± 0.2 vs. control 1.4 ± 0.2) (**Figures 4E through 4G**)

The structural impairment of diabetic microvasculature blunted the functional response of therapeutic neovascularization: the gain of EF induced by rAAV.Tβ4 treatment was less pronounced in the db compared to the wt group (**Figures 5A and 5B, Online Figure 2A**). Consistently, the rise in LV end-diastolic pressure observed in untreated ischemic animals

(**Figure 5C, Online Figure 2B**) was reversed after rAAV.Tβ4 treatment in either background (**Figures 5C and 5D**). Moreover, the level of regional myocardial function in the nonischemic area under rapid pacing was significantly reduced in diabetic hearts (db 8.8 ± 1.2 % vs. wt 16.7 ± 1.0%) (**Figure 5E**). In the ischemic region, recovery upon rAAV.Tβ4 treatment was present in db hearts (8.5 ± 1.4% vs. 1.9 ± 0.8% in untreated db hearts), but significantly less pronounced than in wt hearts (rAAV.Tβ4 16.0 ± 1.2%) (**Figure 5F**). In the ischemic region of db hearts, rAAV.VEGF-A did not alter functional reserve (2.9 ± 0.7%) (**Online Figure 2C**).

Since the complex myovascular interaction in diabetic hearts destabilized microvessels and inhibited therapeutic vessel growth, we investigated the Ang1/Ang2 ratio in the ischemic hearts. The reduced Ang1/Ang2 ratio in ischemic tissue was enhanced upon Tβ4 overexpression in wt as well as db hearts (**Figure 6A, Online Figure 1C**). However, rAAV.VEGF-A application did not improve the Ang1/Ang2 ratio, pointing to the lack of mature microvascular growth. In addition, we investigated the alterations in micro ribonucleic acid (miR), which might account for the pleiotropic actions induced by the hyperglycemic state. Three vasoactive miRs were found upregulated in the hyperglycemic hearts (**Online Figure 3**): miR 26a, which is implicated in impaired wound healing angiogenesis in DM (22); miR92a, a known inhibitor of cardiac angiogenesis (23,24); and miR133a, whose level was previously reported to be elevated in diabetic hearts (25). We found these 3 miRs significantly upregulated in the porcine diabetic hearts (**Online Figure 3**), suggesting them as potential novel mediators of microvascular rarefaction in DM. Furthermore, fibrosis was induced in the ischemic tissue (db 22.5 ± 1.0% vs. wt 19.0 ± 0.8%) (**Figures 6B and 6C**). rAAV.Tβ4 application significantly reduced fibrosis in db as well as wt hearts (13.1 ± 0.6 % and 11.0 ± 0.4%, respectively) (**Figure 6B and 6C**).

DISCUSSION

In the current study, we assessed the impact of cardiovascular risk factors on the induction of vascular growth in the micro- and macrovascular compartment. We found that diabetic human hearts displayed capillary rarefaction and pericyte loss, accompanied by decreased contractility and increased stiffness (**Figure 1**). Moreover, hyperglycemia attenuated tube formation, migration, and pericyte attraction upon proangiogenic stimulation in vitro (**Figure 2**). In vivo, untreated DM induced microcirculatory rarefaction (**Figure 3**) and a distinct functional cardiac impairment in a transgenic *INS*^{C94Y} pig model. Induction of regional chronic ischemia impaired microvascular density in both hyper- and normoglycemic hearts, without functional collateralization of the ischemic region (**Figure 4**). Forced angiogenesis via rAAV.VEGF-A, without concomitant vessel maturation, had no significant effect on regional and global function at rest and under rapid pacing (**Figures 4 and 5**). However, balanced vascular growth was induced via rAAV.Tβ4 in db pig hearts, though to a significantly lesser extent than in wt hearts (**Figure 4**). Functional impairment of hibernating myocardium was improved in db hearts upon Tβ4 treatment, albeit not to the same extent as in normoglycemic hearts (**Figure 5**). MiR analysis of db hearts revealed increased concentrations of antiangiogenic miR 26a, 92a, and 133a. Additionally, a higher degree of fibrosis was observed, which was partially reversed by Tβ4 and VEGF-A (**Figure 6**, **Online Figure 3**). The **Central Illustration** depicts the specific microcirculatory alterations of DM and the effects of Tβ4 and VEGF-A.

Notably, uncontrolled diabetes with continuously elevated glucose levels (**Figure 3A**) itself suffices to rarefy microcirculatory density of cardiac muscle. Capillary loss and pericyte dropout have been well described in the retina (26), but are revealed for the first time in transgenic db pig hearts and in hearts from patients with diabetes. Previously, microvessel destabilization has been attributed to Ang2 overexpression (27). A partial inhibitor of the Tie2

receptor, Ang2 might destabilize microvessels by antagonizing the Ang1/Tie2 interaction, which provides a quiescent and mature vessel state. This feature has been attributed to inflammatory destabilization of microvessels in sepsis (28), but may also occur in chronic inflammatory endothelial activation (26) or in streptozotocin-induced experimental DM (29). Notably, increased Ang2 expression has been found in aged db/db mice characterized by capillary rarefaction and fibrosis (30). In our study, the ratio of Ang1/Ang2 was slightly, but not significantly, decreased in db pig and human hearts compared to normoglycemic hearts (**Figures 1D and 6A**, **Online Figure 1C**), but increased upon rAAV.Tβ4 treatment. In the human tissue, Tβ4 expression was unaltered even though DM human corneas display a distinct Tβ4 reduction (31). However, the vascular growth induction by Tβ4 was previously found to be sensitive to Ang2 (16). Thus, an improved Ang1/Ang2 ratio appears crucial for the balanced vascular growth provided by rAAV.Tβ4.

Interestingly, rAAV.VEGF-A had no effect on the Ang1/Ang2 ratio (**Figure 6A**, **Online Figure 1C**). This was consistent with our previous observation in normoglycemic chronic ischemic pig hearts (15), where rAAV.VEGF-A did not yield sufficient microvessel maturation nor macrovessel growth (arteriogenesis) for functional improvement in our hibernating myocardium model. Lack of microvessel maturation was found critical, since addition of placenta-derived growth factor B to VEGF-A sufficed to induce augmentation of micro- and macro-vessels as well as functional improvement (15).

With rAAV.Tβ4 treatment, we found a decrease of $CD14^+$ monocytes, representing the proinflammatory M1 phenotype, in normo- as well as hyperglycemic pig hearts (**Online Figure 1D**). One potential signal triggering continuous inflammation is increased binding of advanced glycation endproducts to their receptor (RAGE) (14). Besides its intracellular pro-inflammatory

signaling and high mobility group box 1- and nuclear facto κB-dependent upregulation of adhesion molecules (32), cytokines, and chemokines, RAGE itself interacts with Mac-1 on circulating leukocytes, mediating firm adhesion (33,34) and further inflammatory stimulation. Moreover, in metabolic stress (like DM) endosomal damage-associated molecular patterns may activate the inflammasome for a perpetual inflammatory state (35). Finally, miR alterations may take a toll of microvascular preservation. In this respect, miR 92a, miR 26a, and miR133b have shown a distinct increase in hyperglycemia (**Online Figure 3**), which may indicate their involvement in diabetic vascular rarefaction and suggest them as potential therapeutic targets for miR inhibitors (24).

STUDY LIMITATIONS. In this study, we used a transgenic pig model of insulin-dependent DM to investigate the efficacy of vascular gene therapy using rAAV.Tβ4 and rAAV.VEGF-A as therapeutic agents. Thus, we analyzed an untreated cardiac risk factor, representing a 'worst case' scenario for a potential loss of treatment function. We assume that most patients of the target population receive current medical treatment schemes, blunting the described loss of efficacy. Nevertheless, comorbidities like DM must be taken into account when calculating the size of a potential treatment effect.

CONCLUSIONS

We used a transgenic diabetic pig model to quantify vessel growth and functional improvement in hibernating myocardium subjected to rAAV.Tβ4 therapy to improve neovascularization. Our results indicated an attenuated, but still significant, increase of micro- and macro-vessels that improved myocardial function. Thus, we concluded that in the presence of diabetes mellitus, balanced vascular gene therapy, targeting microvascular maturation and macrovascular growth in

addition to angiogenesis, is effective, although not to the same extent as in healthy wild-type animals.

PERSPECTIVES

Competency in Medical Knowledge: In a transgenic, porcine model of diabetes mellitus (InsC94Y), microcirculatory instability compromises myocardial function and angiogenesis.

Translational Outlook: Future research should seek ways to promote capillary stability in patients with diabetes, as this may help preserve myocardial function and reduce myocardial ischemia.

REFERENCES

1. Kannel WB. The Framingham Study: ITS 50-year legacy and future promise. J Atheroscler Thromb 2000;6:60-6.
2. Kim J-J, Hwang B-H, Choi IJ, et al. Impact of diabetes duration on the extent and severity of coronary atheroma burden and long-term clinical outcome in asymptomatic type 2 diabetic patients: evaluation by Coronary CT angiography. Eur Heart J Cardiovasc Imaging 2015;16:1065-73.
3. Bittner V, Bertolet M, Barraza FR, et al. Comprehensive Cardiovascular Risk Factor Control Improves Survival: The BARI 2D Trial. J Am Coll Cardiol 2015;66:765-73.
4. Everett BM, Brooks MM, Vlachos HE, Chaitman BR, Frye RL, Bhatt DL. Troponin and Cardiac Events in Stable Ischemic Heart Disease and Diabetes. N Engl J Med 2015;373:610-20.
5. Baber U, Mehran R, Giustino G, et al. Coronary Thrombosis and Major Bleeding After PCI With Drug-Eluting Stents: Risk Scores From PARIS. J Am Coll Cardiol 2016;67:2224-34.
6. Schoos MM, Dangas GD, Mehran R, et al. Impact of Hemoglobin A1c Levels on Residual Platelet Reactivity and Outcomes After Insertion of Coronary Drug-Eluting Stents (from the ADAPT-DES Study). Am J Cardiol 2016;117:192-200.
7. Nyström T, Holzmann MJ, Eliasson B, Kuhl J, Sartipy U. Glycemic Control in Type 1 Diabetes and Long-Term Risk of Cardiovascular Events or Death After Coronary Artery Bypass Grafting. J Am Coll Cardiol 2015;66:535-43.
8. Klempfner R, Elis A, Matezky S, et al. Temporal trends in management and outcome of diabetic and non-diabetic patients with acute coronary syndrome (ACS): residual

risk of long-term mortality persists: Insights from the ACS Israeli Survey (ACSIS) 2000-2010. Int J Cardiol 2015;179:546-51.

9. Schuster A, Morton G, Chiribiri A, Perera D, Vanoverschelde JL, Nagel E. Imaging in the Management of Ischemic Cardiomyopathy: Special Focus on Magnetic Resonance. J Am Coll Cardiol 2012;59:359-70.

10. [No authors listed] BARI Investigators. The final 10-year follow-up results from the BARI randomized trial. J Am Coll Cardiol 2007;49:1600-6.

11. Rosenson RS, Fioretto P, Dodson PM. Does microvascular disease predict macrovascular events in type 2 diabetes? Atherosclerosis 2011;218:13-8.

12. Orasanu G, Plutzky J. The Pathologic Continuum of Diabetic Vascular Disease. J Am Coll Cardiol 2009;53:S35-S42.

13. Hammes H-P, Feng Y, Pfister F, Brownlee M. Diabetic Retinopathy: Targeting Vasoregression. Diabetes 2011;60:9-16.

14. Shoji T, Koyama H, Morioka T, et al. Receptor for Advanced Glycation End Products Is Involved in Impaired Angiogenic Response in Diabetes. Diabetes 2006;55:2245-55.

15. Kupatt C, Hinkel R, Pfosser A, et al. Cotransfection of Vascular Endothelial Growth Factor-A and Platelet-Derived Growth Factor-B Via Recombinant Adeno-Associated Virus Resolves Chronic Ischemic Malperfusion: Role of Vessel Maturation. J Am Coll Cardiol 2010;56:414-22.

16. Hinkel R, Trenkwalder T, Petersen B et al. MRTF-A controls vessel growth and maturation by increasing the expression of CCN1 and CCN2. Nat Commun 2014;5.

17. Bongiovanni D, Ziegler T, D'Almeida S, et al. Thymosin beta4 attenuates microcirculatory and hemodynamic destabilization in sepsis. Expert Opin Biol Ther 2015;15 Suppl 1:S203-10.

18. Renner S, Braun-Reichhart C, Blutke A et al. Permanent Neonatal Diabetes in INSC94Y Transgenic Pigs. Diabetes 2013;62:1505-11.

19. Bish LT, Morine K, Sleeper MM, et al. AAV9 provides global cardiac gene transfer superior to AAV1, AAV6, AAV7, and AAV8 in the mouse and rat. Hum Gene Ther 2008;19:1359-68.

20. Kupatt C, Hinkel R, von Bruhl ML, et al. Endothelial nitric oxide synthase overexpression provides a functionally relevant angiogenic switch in hibernating pig myocardium. J Am Coll Cardiol 2007;49:1575-84.

21. Kupatt C, Hinkel R, von Bruhl ML, et al. Endothelial nitric oxide synthase overexpression provides a functionally relevant angiogenic switch in hibernating pig myocardium. J Am Coll Cardiol 2007;49:1575-84.

22. Icli B, Nabzdyk CS, Lujan-Hernandez J, et al. Regulation of impaired angiogenesis in diabetic dermal wound healing by microRNA-26a. J Mol Cell Cardiol 2016;91:151-9.

23. Bonauer A, Carmona G, Iwasaki M, et al. MicroRNA-92a Controls Angiogenesis and Functional Recovery of Ischemic Tissues in Mice. Science 2009:1174381.

24. Hinkel R, Penzkofer D, Zuehlke S, et al. Inhibition of MicroRNA-92a Protects Against Ischemia-Reperfusion Injury in a Large Animal Model. Circulation 2013;128:1066-75.

25. Fichtlscherer S, Zeiher AM, Dimmeler S. Circulating microRNAs: biomarkers or mediators of cardiovascular diseases? Arterioscler Thromb Vasc Biol 2011;31:2383-90.

26. Hammes HP, Du X, Edelstein D, et al. Benfotiamine blocks three major pathways of hyperglycemic damage and prevents experimental diabetic retinopathy. Nat Med 2003;9:294-9.

27. Hammes HP, Lin J, Wagner P, et al. Angiopoietin-2 Causes Pericyte Dropout in the Normal Retina: Evidence for Involvement in Diabetic Retinopathy. Diabetes 2004;53:1104-10.

28. Ziegler T, Horstkotte J, Schwab C, et al. Angiopoietin 2 mediates microvascular and hemodynamic alterations in sepsis. J Clin Invest 2013;123:3436-45.

29. Tuo QH, Zeng H, Stinnett A, et al. Critical role of angiopoietins/Tie-2 in hyperglycemic exacerbation of myocardial infarction and impaired angiogenesis. Am J Physiol Heart Circ Physiol 2008;294:H2547-57.

30. Gonzalez-Quesada C, Cavalera M, Biernacka A, et al. Thrombospondin-1 Induction in the Diabetic Myocardium Stabilizes the Cardiac Matrix in Addition to Promoting Vascular Rarefaction Through Angiopoietin-2 Upregulation. Circ Res 2013;113:1331-44.

31. Saghizadeh M, Kramerov AA, Tajbakhsh J, et al. Proteinase and Growth Factor Alterations Revealed by Gene Microarray Analysis of Human Diabetic Corneas. Invest Ophthalmol Vis Sci 2005;46:3604-15.

32. Schmidt AM, Hori O, Chen JX, et al. Advanced glycation endproducts interacting with their endothelial receptor induce expression of vascular cell adhesion molecule-1

(VCAM-1) in cultured human endothelial cells and in mice. A potential mechanism for the accelerated vasculopathy of diabetes. J Clin Invest 1995;96:1395-403.

33. Frommhold D, Kamphues A, Hepper I, et al. RAGE and ICAM-1 cooperate in mediating leukocyte recruitment during acute inflammation in vivo. Blood 2010;116:841-9.

34. Ziegler T, Horstkotte M, Lange P, et al. Endothelial RAGE exacerbates acute postischaemic cardiac inflammation. J Thromb Haemost2016;116:300-8.

35. Chibber R, Ben-Mahmud BM, Mann GE, Zhang JJ, Kohner EM. Protein Kinase C ß2-Dependent Phosphorylation of Core 2 GlcNAc-T Promotes Leukocyte-Endothelial Cell Adhesion: A Mechanism Underlying Capillary Occlusion in Diabetic Retinopathy. Diabetes 2003;52:1519-27.

FIGURE LEGENDS

CENTRAL ILLUSTRATION Tβ4 Gene Therapy and Therapeutic Neovascularization

Diabetes mellitus impairs vascular density in the heart. Proangiogenic gene therapy via Thymosin β4 (Tβ4) or vascular endothelial growth factor-A (VEGF-A) induces capillary growth in diabetic heart. However, only Tβ4 is capable of inducing therapeutic neovascularization via vessel growth and maturation, thereby improving perfusion and myocardial function in ischemic normal as well as diabetic hearts.

FIGURE 1 DM Alters Cardiac Function

(A) Tissue samples of patients with diabetes mellitus (DM) undergoing heart transplantation display capillary rarefaction. **(B)** Besides a reduced capillary density (PECAM-1+), **(C)** these patients demonstrated a loss of pericytes (NG2+). **(D)** DM status did not change expression of Thymosin β4 (Tβ4) in the human cardiac tissue of end-stage heart failure patients. The ratio of angiopoietin (Ang) 1 and 2 expression was reduced patients with DM. **(E)** Force development of human cardiac tissue slides revealed a reduced contractile function in DM patients undergoing heart transplantation. **(F)** Ventricular stiffness is impaired in DM heart slices compared to non-DM samples. Mean ± SEM; n = 4; *$p < 0.05$. hpf = high power field; PECAM-1 = platelet endothelial cell adhesion molecule-1.

FIGURE 2 High Glucose Levels Alter Proangiogenic Effects

(A) Tube formation capacity of murine endothelial cells is altered under high-glucose levels; Tβ4 and vascular endothelial growth factor-A (VEGF-A) transfection enhanced tube formation under normo- and high-glucose levels (scale bar = 200 μm). **(B)** Similarly, high glucose reduced endothelial cell migration in vitro in a wound-scratch assay (red area = uncovered area; scale bar = 200 μm) while Tβ4 or VEGF-A overexpression enhanced migration capacity in normo- and

high-glucose conditions. **(C and D)** High-glucose levels reduced tube maturation, assessed as pericyte recruitment (green fluorescence) to endothelial rings (red fluorescence; scale bar = 100 μm); transfection of Tβ4, but not VEGF-A, enhanced maturation at normo- and high-glucose levels. **(E)** High-glucose levels increased adhesion of human monocytic THP-1 cells under venular shear stress (4 dyn/s; scale bar = 100 μm); Tβ4 transfection reduced this endothelium-leukocyte interaction in normo- and high-glucose levels. Mean ± SEM; n = 3. *p < 0.05; **p < 0.001. Abbreviations as in Figure 1.

FIGURE 3 Capillary Rarefaction

(A) Fasted blood glucose levels are enhanced in the transgenic diabetic (db) pigs (C94Y mutation in the porcine insulin gene) compared to the wild-type (wt) littermates. In cardiac tissue, **(B and C)** capillary density (PECAM-1+) as well as **(B and D)** vessel integrity (NG2+) were reduced in the transgenic db versus wt pigs. **(E and F)** Fibrosis (scale bar = 100 μm) was significantly increased in db hearts. Transgenic db pig also demonstrated **(G)** reduced ejection fraction (EF) and **(H)** diminished contractile functional reserve assessed by subendothelial sonomicrometry at rest and rapid atrial pacing (120 and 150 beats/min). **(I)** Left ventricular end-diastolic pressure (LVEDP) increased under high-glucose conditions in db pigs. Mean ± SEM; n = 4. *p < 0.05; **p < 0.001. SES = subendocardial segment shortening; other abbreviations as in Figures 1 and 2.

FIGURE 4 DM Relevance for Vascularization in Chronic Myocardial Ischemia

(A) Fasted blood glucose levels are enhanced in db pigs at days 0, 28, and 56 versus their age-matched wt littermates. Chronic myocardial ischemia leads to **(B and C)** capillary rarefaction (PECAM-1+) in both wt and db pig hearts. The reduced capillary number is associated with **(B and D)** a loss of pericytes (NG2+) in the ischemic tissue in both control groups. This effect was

at least partially reversed after rAAV.Tβ4 transduction, less so in db animals, an effect not observed after rAAV.VEGF-A application. **(E)** Representative pictures and **(F)** quantification of collateral growth, measured at day 56, which was enhanced after rAAV.Tβ4 application; rAAV.VEGF-A application showed no cardioprotective effect. **(G)** Perfusion of the vessel distal to the occlusion site, displayed as Rentrop score, revealed a reduced filling in wt and db control animals. Tβ4, but VEGF-A overexpression, was capable of enhancing vessel perfusion. Mean ± SEM; n = 6 to 8. *$p < 0.05$; **$p < 0.001$. rAAV = recombinant adeno-associated virus; other abbreviations as in Figures 1, 2, and 3.

FIGURE 5 Tβ4-induced Cardioprotection

(A) Systolic myocardial function, measured by EF, improved in rAAV.Tβ4-transduced but not rAAV.VEGF-A treated animals at day 56. **(B)** Change from day 28 to 56 (ΔEF) showed comparable changes in wt and db rAAV.Tβ4 animals, although at different levels. **(C)** LVEDP increased in wt and db ischemic hearts day 28 to 56, unless Tβ4 was overexpressed. VEGF-A transduction did not reduce the enhanced LVEDP in the ischemic db hearts. **(D)** Change from day 28 to 56 (ΔLVEDP) showed similar effects in wt and db rAAV.Tβ4 animals, but at different levels. **(E)** Functional reserve in the nonischemic (left anterior descending region) tissue is diminished in db hearts compared to normo-glycemic animals. **(G)** In the ischemic (ramus circumflexus region), rAAV.Tβ4 application enhanced myocardial contractile function in both wt and db animals, while rAAV.VEGF-A showed no protective effect. Mean ± SEM; n = 6 to 8. *$p < 0.05$; ** $p < 0.001$. Abbreviations as in Figures 1, 2, 3, and 4.

FIGURE 6 DM-induced Molecular Alterations

(A) Ang1/Ang2 expression improved after Tβ4 but not VEGF-A transduction in both wt and db animals. **(B and C)** Chronic myocardial ischemia-induced fibrosis (scale bar = 100 μm) is

accelerated under diabetic conditions (wt control vs. db control). Overexpression of Tβ4 or VEGF-A significantly reduced fibrosis in the ischemic tissue in both wt and db hearts. Mean ± SEM; n = 6 to 8 for fibrosis. *$p < 0.05$; **$p < 0.001$. Abbreviations as in Figures 1, 3, and 4.

Wild-type Normoxia

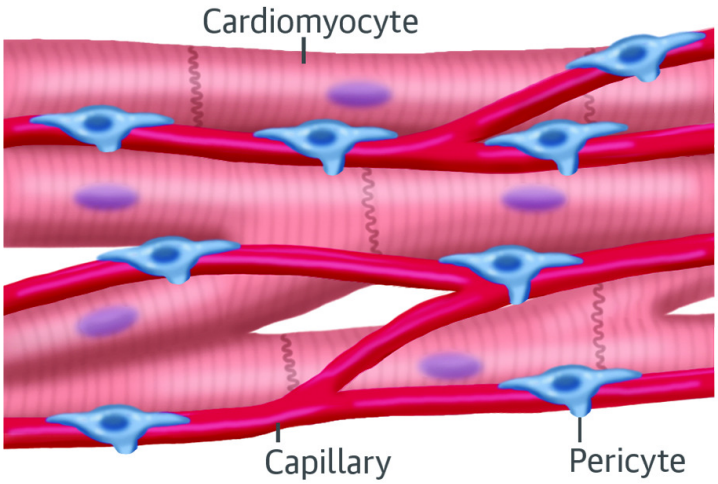

Diabetes Mellitus Ischemia

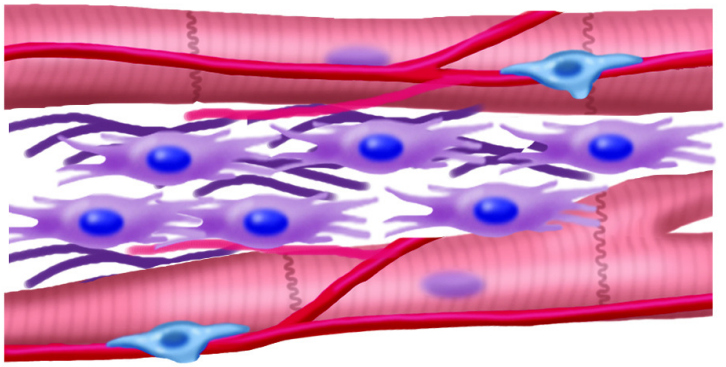

Diabetes Mellitus Ischemia + rAAV.Tß4

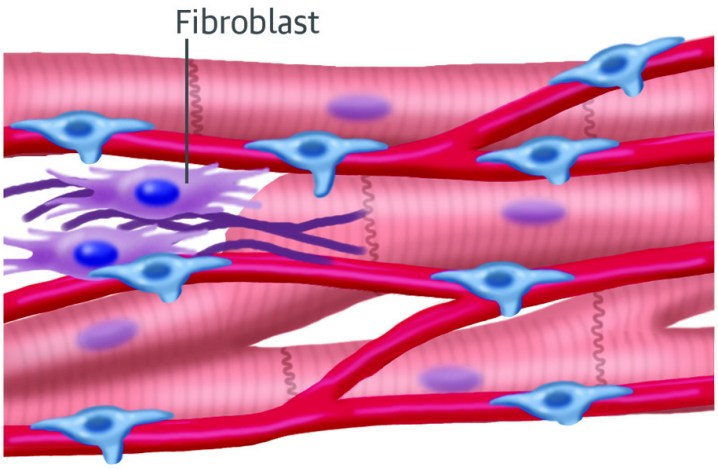

Diabetes Mellitus Ischemia + rAAV.VEGF-A

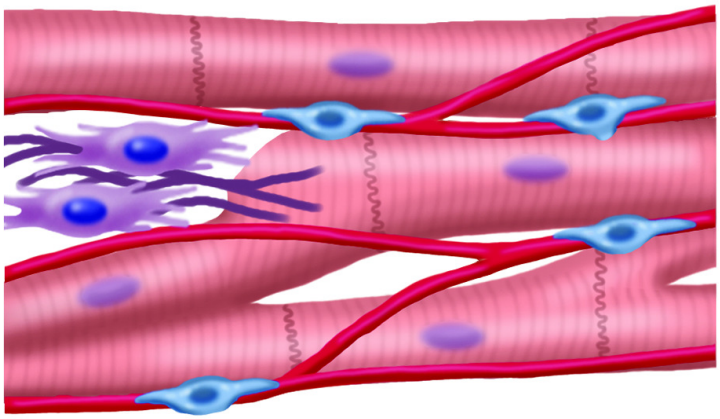

Figure 1

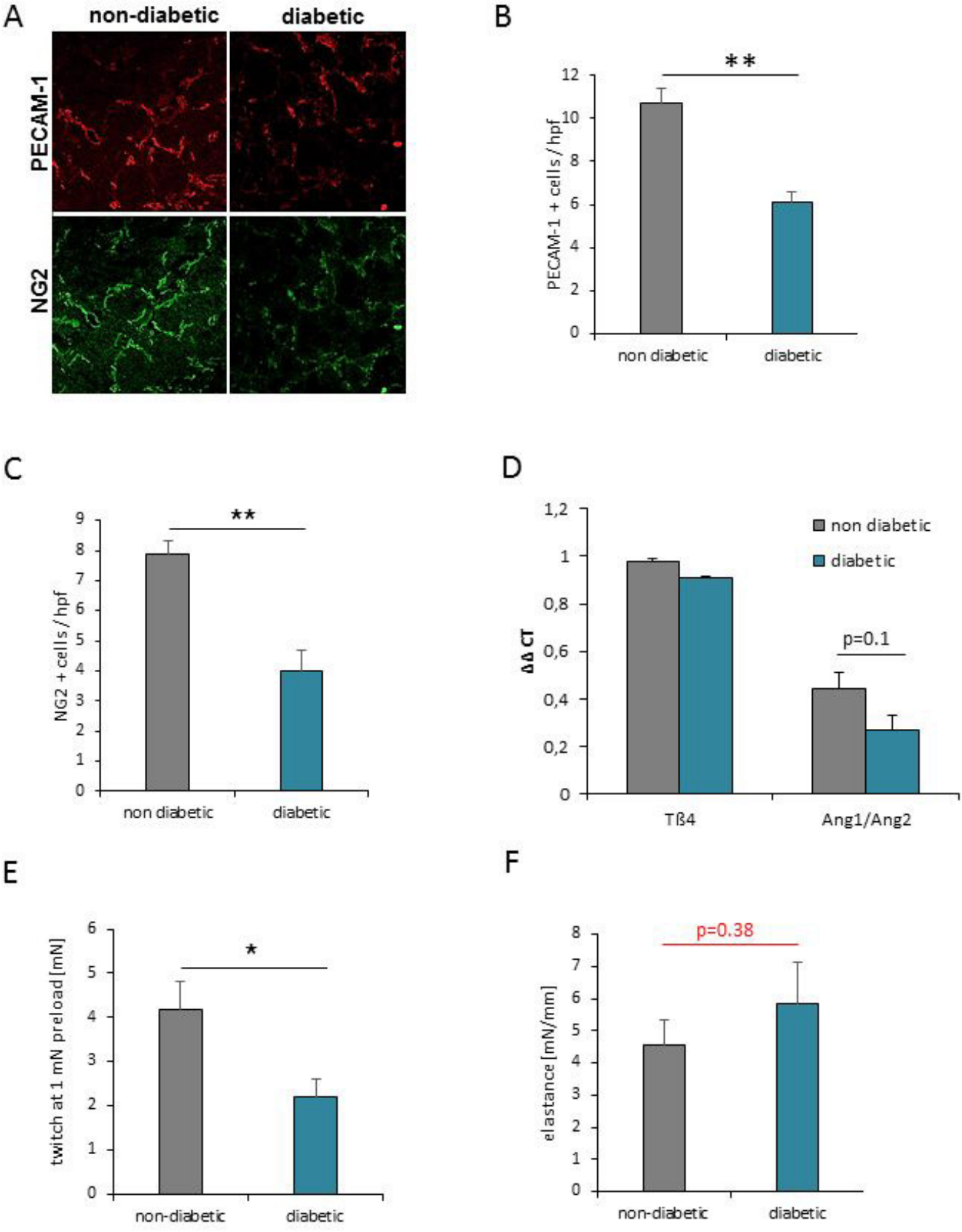
A
non-diabetic
diabetic
PECAM-1
NG2
B
**
PECAM-1 + cells / hpf
non diabetic
diabetic
C
**
NG2 + cells / hpf
non diabetic
diabetic
D
non diabetic
diabetic
ΔΔ CT
p=0.1
Tß4
Ang1/Ang2
E
*
twitch at 1 mN preload [mN]
non-diabetic
diabetic
F
p=0.38
elastance [mN/mm]
non-diabetic
diabetic

Figure 2

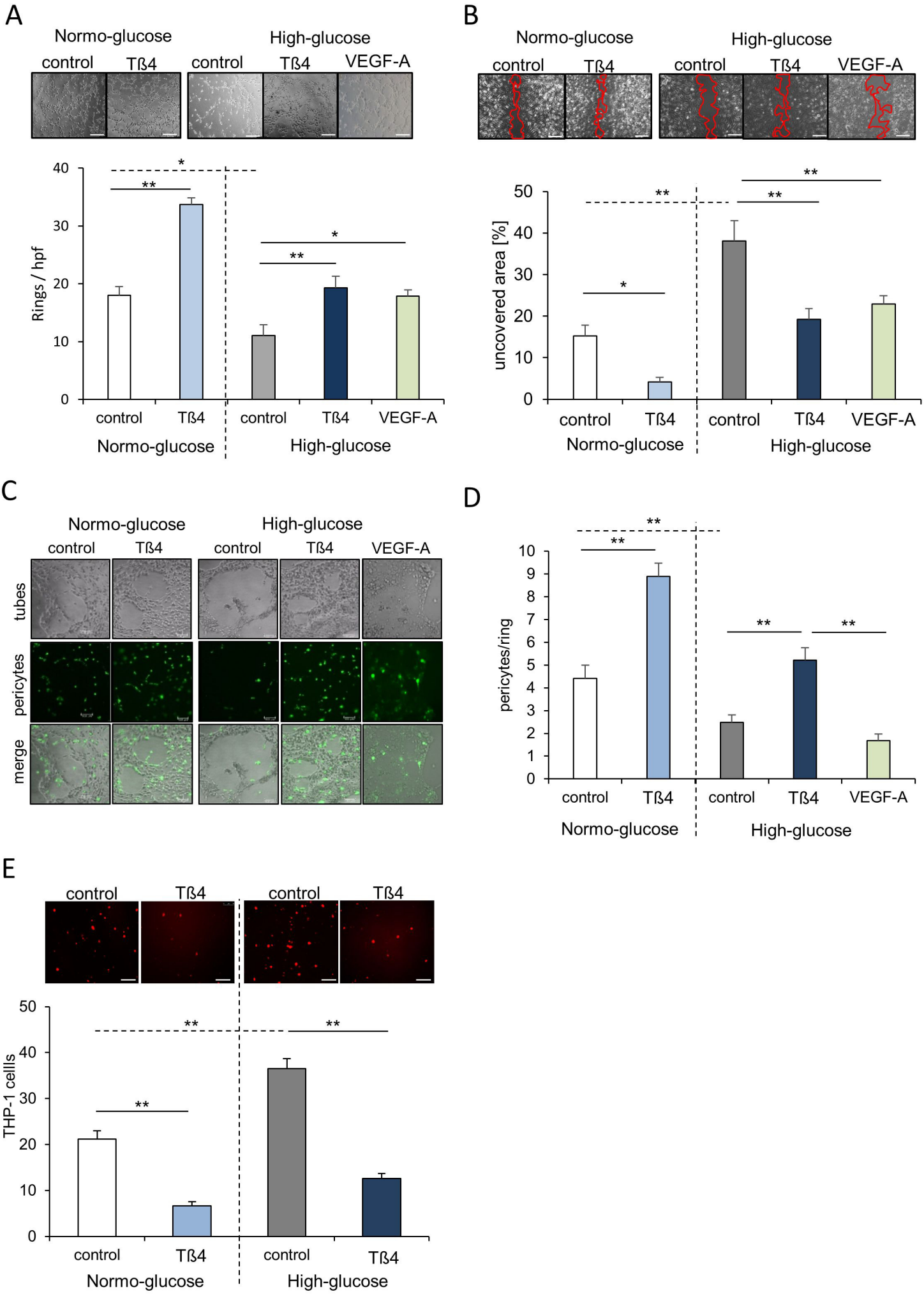
A
Normo-glucose
High-glucose
control
Tß4
control
Tß4
VEGF-A
Rings / hpf
40
30
20
10
0
*
**
*
**
control
Tß4
control
Tß4
VEGF-A
Normo-glucose
High-glucose
B
Normo-glucose
High-glucose
control
Tß4
control
Tß4
VEGF-A
uncovered area [%]
50
40
30
20
10
0
**
**
**
*
control
Tß4
control
Tß4
VEGF-A
Normo-glucose
High-glucose
C
Normo-glucose
High-glucose
control
Tß4
control
Tß4
VEGF-A
tubes
pericytes
merge
D
pericytes/ring
10
9
8
7
6
5
4
3
2
1
0
**
**
**
**
control
Tß4
control
Tß4
VEGF-A
Normo-glucose
High-glucose
E
control
Tß4
control
Tß4
THP-1 cellls
50
40
30
20
10
0
**
**
**
control
Tß4
control
Tß4
Normo-glucose
High-glucose

Figure 3

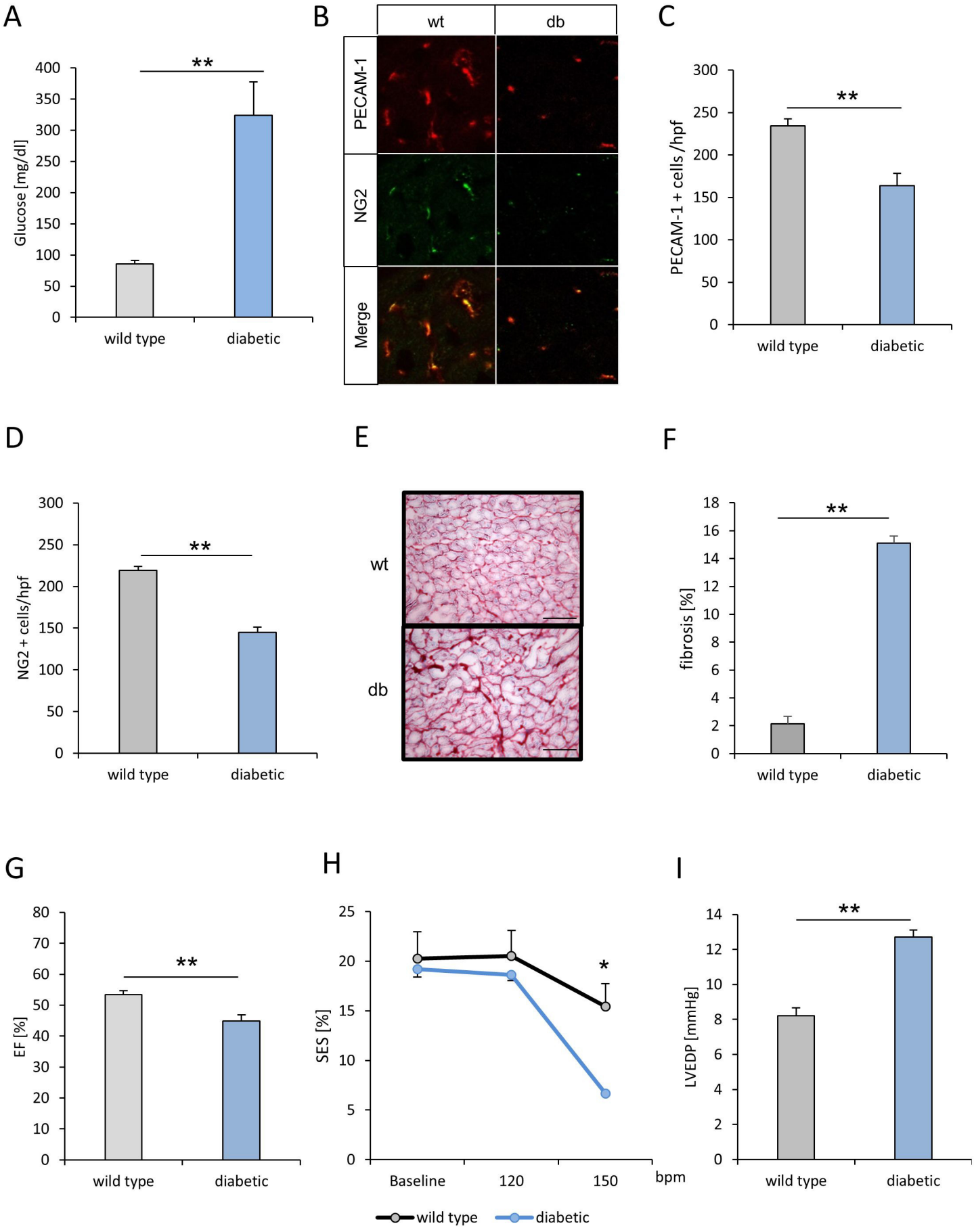
A
Glucose [mg/dl]
400
350
300
250
200
150
100
50
0
**
wild type
diabetic
B
wt
db
PECAM-1
NG2
Merge
C
PECAM-1 + cells /hpf
300
250
200
150
100
50
0
**
wild type
diabetic
D
NG2 + cells/hpf
300
250
200
150
100
50
0
**
wild type
diabetic
E
wt
db
F
fibrosis [%]
18
16
14
12
10
8
6
4
2
0
**
wild type
diabetic
G
EF [%]
80
70
60
50
40
30
20
10
0
**
wild type
diabetic
H
SES [%]
25
20
15
10
5
0
*
Baseline
120
150
bpm
wild type
diabetic
I
LVEDP [mmHg]
14
12
10
8
6
4
2
0
**
wild type
diabetic

Figure 4

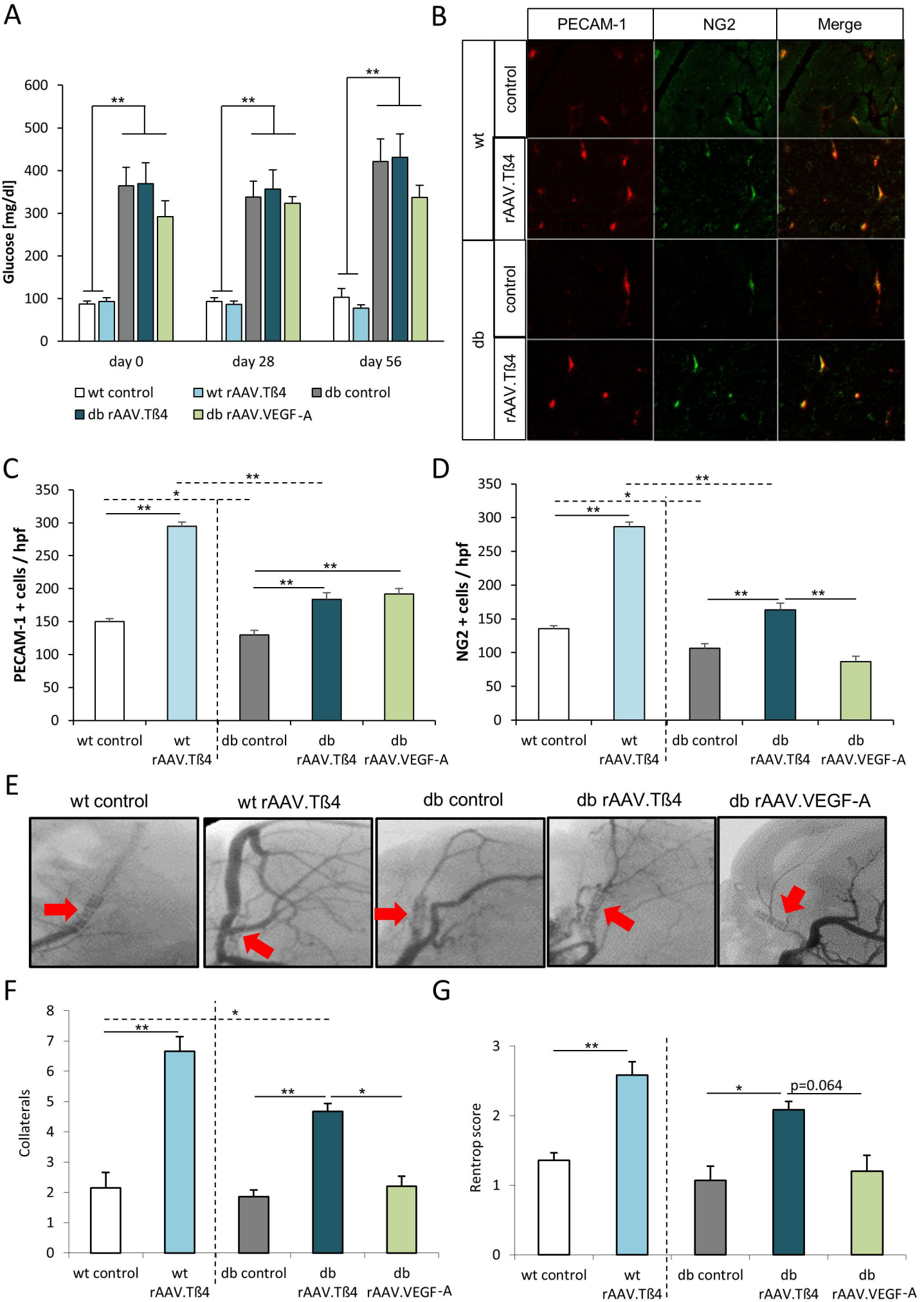
A
Glucose [mg/dl]
day 0
day 28
day 56
wt control
wt rAAV.Tß4
db control
db rAAV.Tß4
db rAAV.VEGF-A
B
PECAM-1
NG2
Merge
wt
db
control
rAAV.Tß4
C
PECAM-1 + cells / hpf
D
NG2 + cells / hpf
E
F
Collaterals
G
Rentrop score
p=0.064

Figure 5

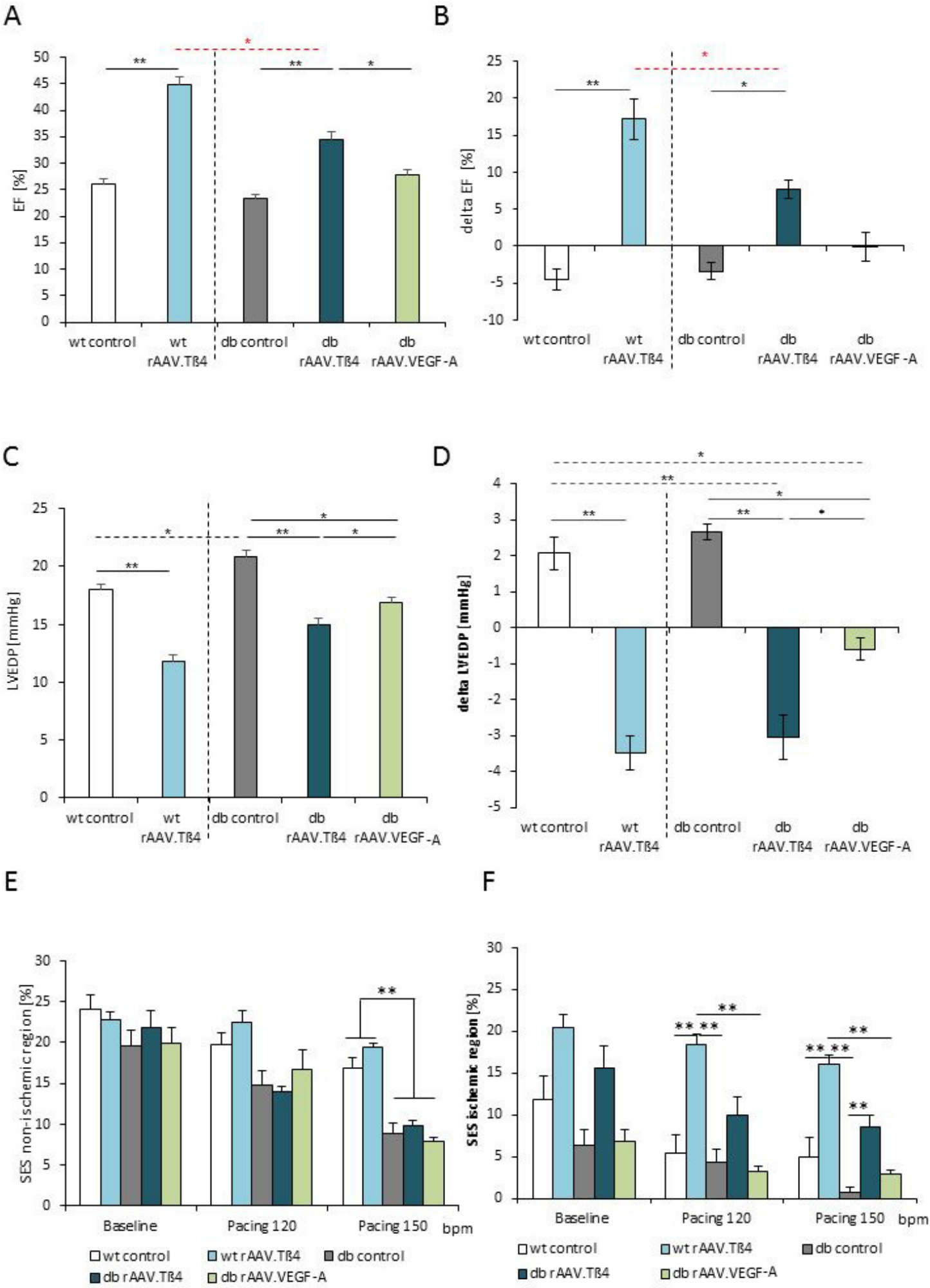
A
EF [%]
wt control
wt rAAV.Tß4
db control
db rAAV.Tß4
db rAAV.VEGF-A
B
delta EF [%]
C
LVEDP [mmHg]
D
delta LVEDP [mmHg]
E
SES non-ischemic region [%]
Baseline
Pacing 120
Pacing 150
bpm
F
SES ischemic region [%]

Figure 6

A

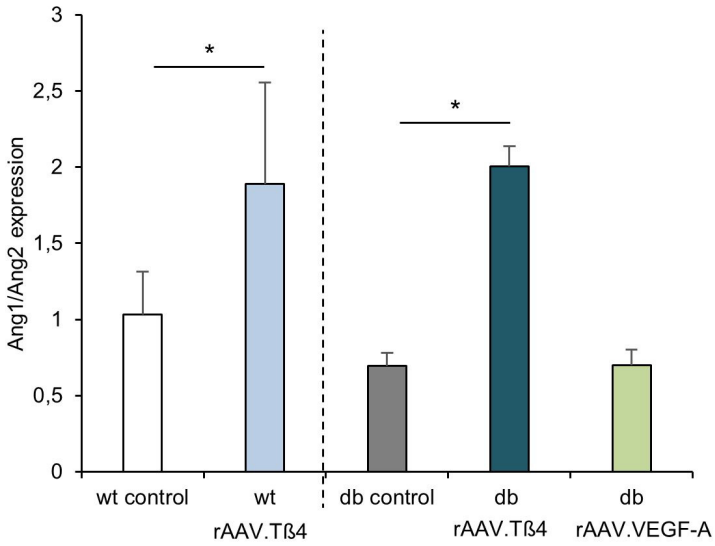
Ang1/Ang2 expression
3
2,5
2
1,5
1
0,5
0
*
*
wt control
wt rAAV.Tß4
db control
db rAAV.Tß4
db rAAV.VEGF-A

B

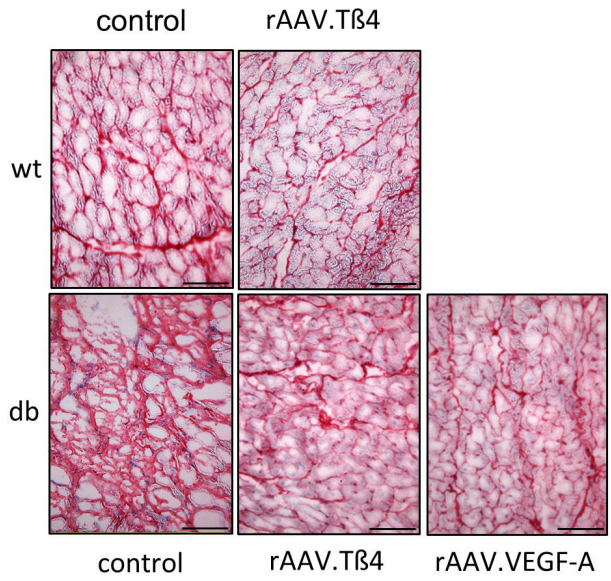
control
rAAV.Tß4
wt
db
control
rAAV.Tß4
rAAV.VEGF-A

C

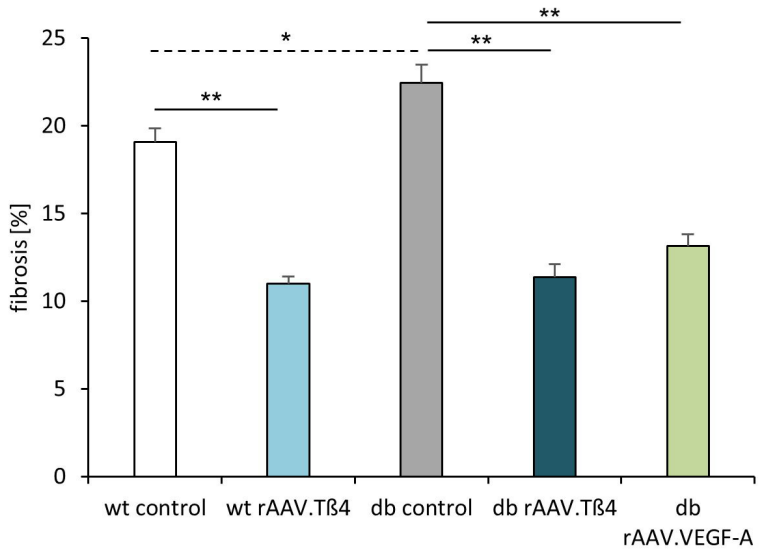
fibrosis [%]
25
20
15
10
5
0
*
**
**
**
wt control
wt rAAV.Tß4
db control
db rAAV.Tß4
db rAAV.VEGF-A

ONLINE APPENDIX

Online Figure 1: A Protocol of the hibernating myocardium model in diabetic and wild-type pigs. **B** RT-PCR detection of virus transduction in heart tissue of control (wt) and diabetic transgenic (db) pigs (ΔΔCT values normalized to control animals). **C** Expression profile of Angiopoietin-1 (Ang-1) and Angiopoietin-2 (Ang-2) showed an increase of Ang-2 expression in the db compared to wt animals, an effect sensitive to Thymosin β4 but not VEGF-A transduction. **D** Analysis of inflammation in the ischemic tissue (CD14 positive cells/low power field), showing a decrease of inflammation after Tß4 overexpression in wt as well as db animals. This effect was not observed after VEGF-A transduction in the db hearts. (Mean ± SEM, n=4, * $p<0.05$, ** $p<0.001$)

Online Figure 2: A Left ventricular end-diastolic pressure (LVEDP) increased in ischemic wt as well as db hearts from day 28 to 56, unless Thymosin β4 was overexpressed. VEGF transduction did not reduce the enhanced LVEDP in the ischemic db hearts. **B** Analysis of ejection fraction revealed an improvement of systolic myocardial function after rAAV.Tβ4 treatment of wt and db animals at day 56. No gain of ejection fraction was found in rAAV.VEGF-A treated hearts. **C** Regional myocardial function is assessed by subendocardial segment shortening at rest and under atrial pacing (120 and 150 bpm). The functional reserve in the ischemic area in relation to the non-ischemic (LAD region) tissue is enhanced after rAAV.Tβ4 application to the same extent in wt and db animals, VEGF-A however, showed no protective effect (Mean ± SEM, n=6-8, * $p<0.05$, ** $p<0.001$).

Online Figure 3: miRNA expression analysis in wt and db non-ischemic heart tissue displayed a significant up-regulation of miRNA-26a, miRNA-92a and miR-199a in diabetes.

Online Table 1

	non-diabetic	**diabetic**
Group size (n)	n=5	n=4
Age (years)	*54±3*	*60±4*
Gender (m/f)	3/2	4/0
Co-morbidities		
ICM	3	2
DCM	2	2
LVAD	1	1

Patient characteristics

From Methods Section

(page numbers from v3)

Page 4

Capillaries were stained with a CD31 (PECAM)-antibody, whereas vessel maturation was quantified by pericyte (NG2 antibody) costaining. Pictures were taken with high-power field magnification (40-fold) and 5 independent pictures per region and animal were quantified.

Fibrosis staining was performed by Sirius red oil staining in nonischemic and ischemic animals (wt and db). Pictures were taken at a 10-fold magnification (low power field). Red fibrotic area in percent was quantified via ImageJ v.1.43u in 5 independent pictures per region.

Pro-inflammatory cells (macrophages) were stained with a CD14 antibody in the ischemic tissue. Pictures again were taken with low power field magnification (10-fold) and 5 independent pictures per region and animal were quantified.

Page 5

Specimens of LV myocardium (4 in the non-DM and 5 in the DM group) were obtained as 2 x 2 cm^2 transmural biopsies from explanted failing hearts at the Heart and Diabetes Center of Northrhine Westphalia, and were immediately placed in cold (4° C) HEPES buffered salt solution containing 30 mM BDM (3-butanedione 2-monoxime). Samples were sent by overnight courier to the Walter-Brendel-Center, Munich, where 300 µm thick tissue slices were prepared within 18 to 31 h after surgery, as previously described (19). Briefly, trimmed tissue blocks were embedded in 4% agarose, mounted onto a vibratome, and cut along the transversal direction proceeding from the endocardial to epicardial layers of the myocardium.

Freshly prepared myocardial slices of 5 x 5 mm^2 surface area were mounted onto a horizontal organ bath, and superfused with gassed Ringer solution (5 % CO_2, 20 % O_2, 37° C) at 4 ml/min as previously described (19).

Pages 5-6

For direct matrigel assays, human umbilical vein endothelial cells (HUVEC) were transfected with pcDNA, Tβ4, or VEGF-A. Cells were diluted to a final density of 10,000 cells/50 µl and seeded on matrigel. Pictures were taken after 18 h. Number of rings per low power field was quantified.

For pericyte co-culture experiments murine endothelial cells (bEnd.3) were transfected with pcDNA, Tβ4, or VEGF-A as described previously. Endothelial cells were stained with DiD (red, Vybrand), diluted to a final density of 10,000 cells/30µl and seeded on matrigel. After 18 h, tube formation was investigated. Murine embryonic pericytes were cultured according the manufacturer´s instructions and added to the pre-formed tubes (1,000 cells/15µl per well, pre-labeled green, DiO, Vybrand). After 6 h of coculture, pictures were taken by confocal laser microscopy and the PC per tube ratio was analyzed.

For detection of leukocyte adhesion shear stress experiments were performed as follows: Ibidi-slides were seeded with HUVEC which were under normo- or high-glucose and transfected with pcDNA or Tβ4. After 24 h, when the cell layer was confluent, THP-1 cells (leukocyte cell line) were superfused at a density of 750,000 cells per ml and at a flow rate of 0.57 ml/min (1 dyn/cm^2). After 8 min of cell superfusion and 2 min of washing with medium only (at the same flow rate), adherent cells were counted.

Pages 6-7

Briefly, transfection of HEK293 cells was performed using 1 plasmid encoding the transgene under control of the CMV promoter flanked by cis acting AAV2 internal terminal repeats, a second plasmid providing AAV2 rep and AAV9 cap in trans, whereas a third plasmid supplemented adenoviral helper function using polyethylenimine. Titers of the rAAVs were determined via quantitative real time polymerase chain reaction (qRT-PCR) against the bGH polyA tail of the vector (primer sequence: forward 5′-TCTAGTTGCCAGCCATCTGTTGT-3′, reverse 5′-TGGGAGTGGCACCTTCCA-3′).

Briefly, ischemia was induced by emplacing a reduction stent (2.5 x 13mm, Jomed, Germany) (22) into the proximal RCx, inducing a 75% stenosis which progressed to total occlusion at day 28 (**Online Figure 1A**). This model is characterized by hibernating myocardium (dysfunctional, but viable and metabolically hyperactive, cf. [22]), functionally responding to improvement of microcirculatory blood flow, as assessed by fluorescent microspheres (16,23). A marker of gradual stent occlusion and an inclusion criterion was an area of infarcted myocardium <6% of total LV area at d56 (tetrazolium-red-staining).

References that now appear only online in support of above material:

19 Brandenburger M, Wenzel J, Bogdan R et al. Organotypic slice culture from human adult ventricular myocardium. Cardiovasc Res 2012;93:50-9.

22 von Degenfeld G, Raake P, Kupatt C, et al. Selective pressure-regulated retroinfusion of fibroblast growth factor-2 into the coronary vein enhances regional myocardial blood flow and function in pigs with chronic myocardial ischemia. J Am Coll Cardiol 2003;42:1120-8.

23 Kupatt C, Hinkel R, Pfosser A, et al. Cotransfection of Vascular Endothelial Growth Factor-A and Platelet-Derived Growth Factor-B Via Recombinant Adeno-Associated Virus Resolves Chronic Ischemic Malperfusion: Role of Vessel Maturation. J Am Coll Cardiol 2010;56:414-22.

Suppl. Figure 1

A

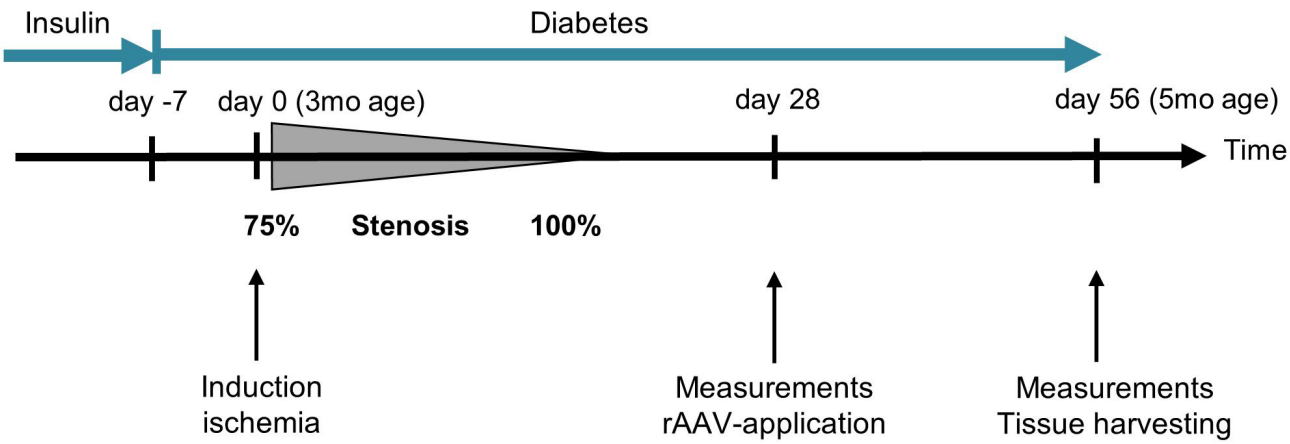

B

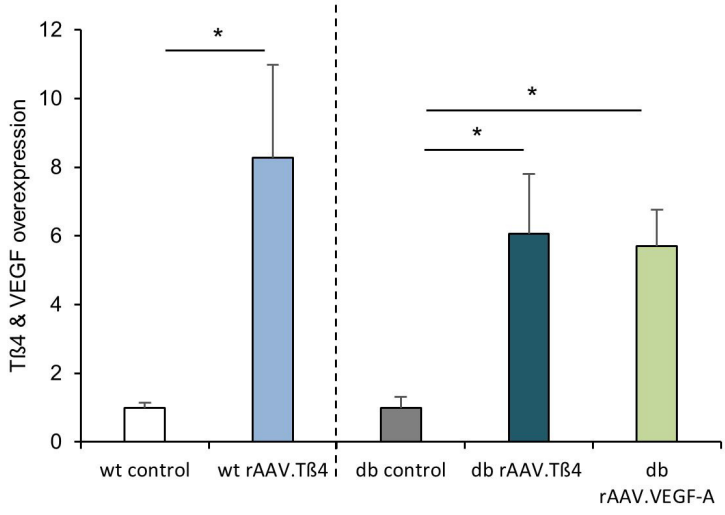

C

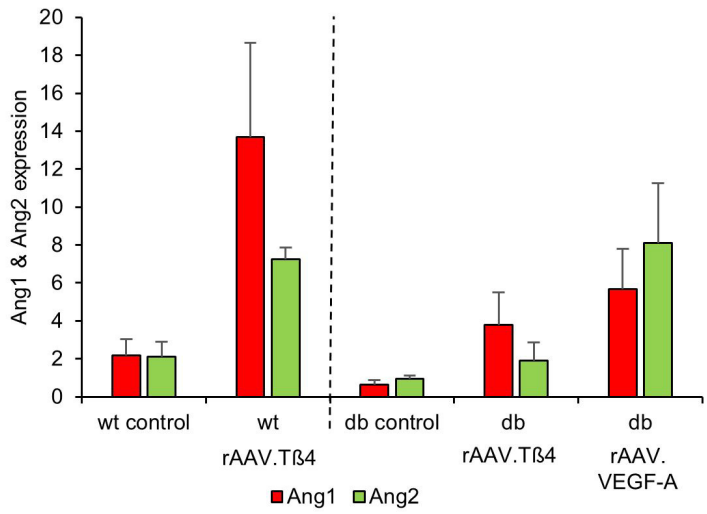

D

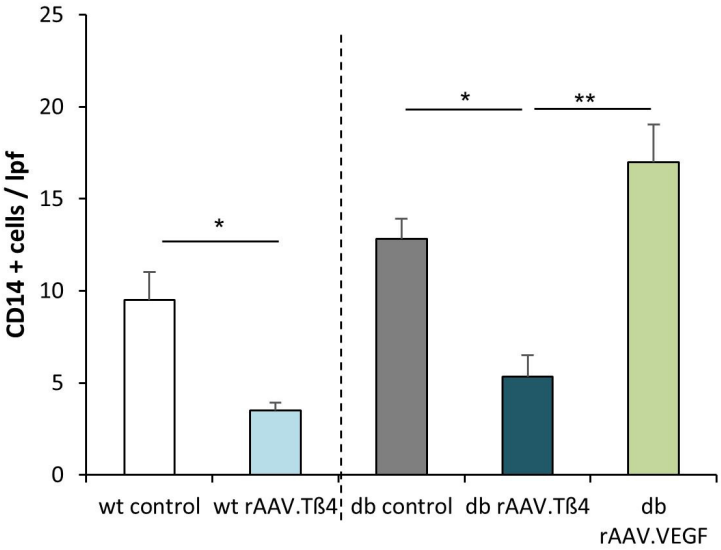

Suppl. Figure 2

A

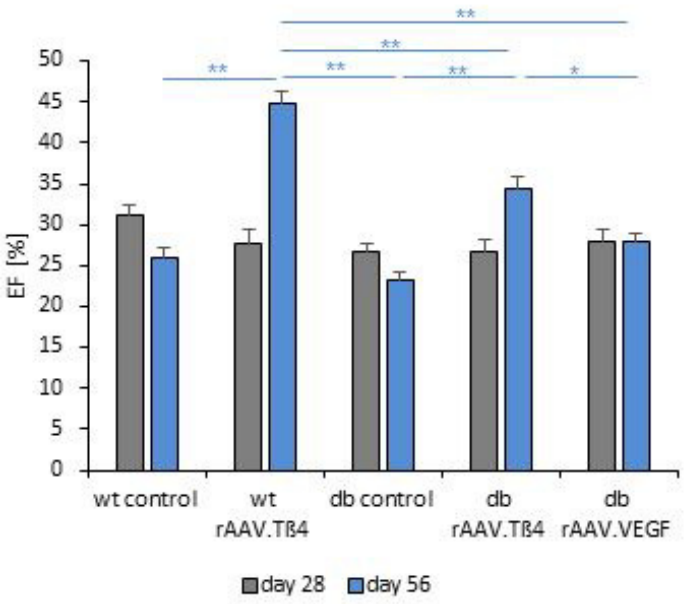

B

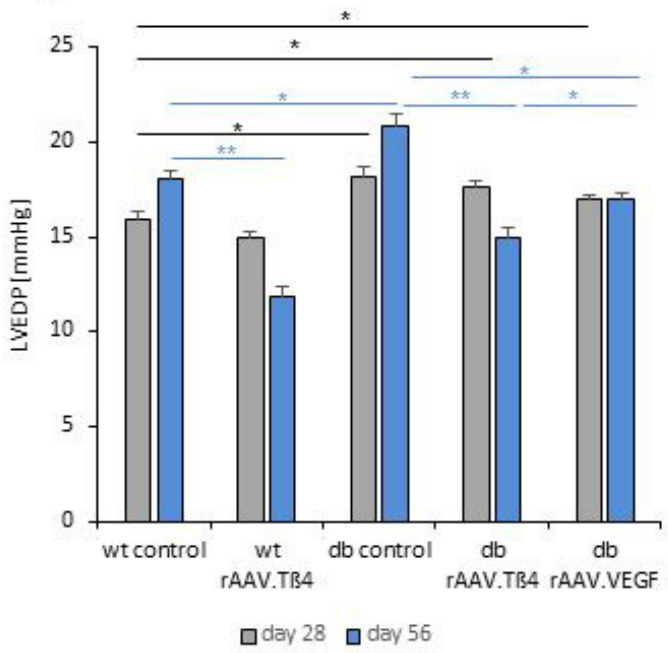

C

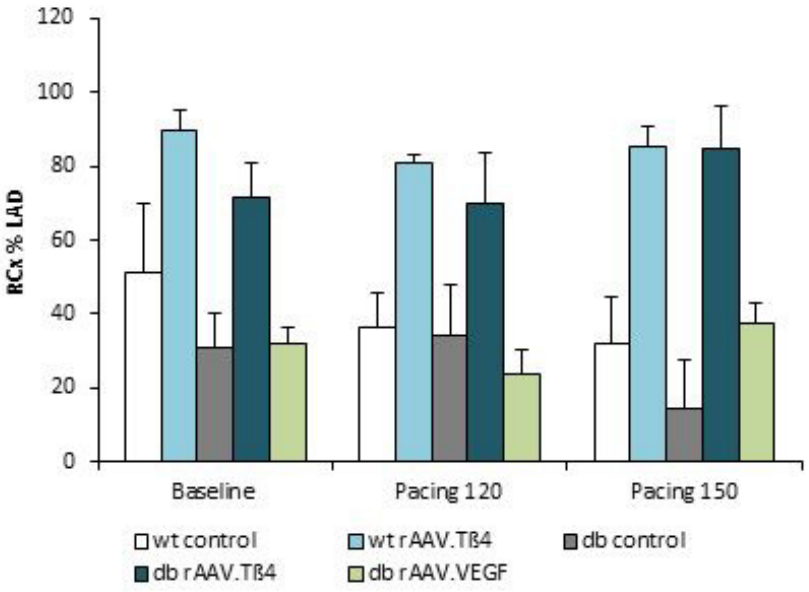

Suppl. Figure 3

A